HHS Public Access

Author manuscript

J Bone Miner Res. Author manuscript; available in PMC 2018 November 01.

Published in final edited form as:

J Bone Miner Res. 2017 November ; 32(11): 2248–2256. doi:10.1002/jbmr.3219.

Multimodality Image-Guided Cryoablation for Inoperable Tumor-Induced Osteomalacia

Sri Harsha Tella[1,5], **Hayet Amalou**[2], **Bradford J Wood**[2], **Richard Chang**[3], **Clara C. Chen**[4], **Cemre Robinson**[5], **Michelle Millwood**[5], **Guthrie Lori**[5], **Sheng Xu**[2], **Elliot Levy**[2], **Venkatesh Krishnasamy**[2], **Rachel I. Gafni**[5], and **Michael T. Collins**[5]

[1]Department of Endocrinology, Diabetes and Metabolism, National Institute of Child Health and Human Development, National Institutes of Health (NICHD/NIH), Bethesda, MD

[2]Interventional Radiology and Center for Interventional Oncology, National Institutes of Health (NIH), Bethesda, MD

[3]Endocrine and Venous Services Section, Radiology and Imaging Sciences, National Institutes of Health, Bethesda, MD

[4]Nuclear Medicine section, National Institutes of Health, Bethesda, MD

[5]Skeletal Clinical Studies Unit, Craniofacial and Skeletal Diseases Branch, National Institute of Dental and Craniofacial Research, National Institutes of Health, Bethesda, MD

Abstract

Tumor-induced osteomalacia (TIO) is a debilitating paraneoplastic condition caused by small phosphaturic mesenchymal tumors (PMTs) that secrete large amounts of the phosphate- and vitamin D-regulating hormone, FGF23. Tumor removal results in cure. However, due to high perioperative comorbidity, either from tumor location or host factors, surgery is sometimes not an option. Tumor destruction via cryoablation may be an effective option for inoperable PMTs. Three subjects with a confirmed diagnosis of TIO were studied. All three underwent cryoablation of suspected PMTs rather than surgery due to significant medical comorbidities or challenging anatomical location. subject #3 had tumor embolization 24-hours prior to cryoablation due to the size and hypervascularity of the tumor. The success of the tumor cryoablation was defined by normalization of serum phosphate and FGF23. Cryoablation resulted in a rapid decrease in plasma intact FGF23 by 24-hours post-procedure in all three subjects (0, 2, and 9 pg/mL, respectively) with normalization of blood phosphate by post-procedure day #3. Day #3 renal tubular reabsorption of phosphate increased to 76%, 94% and 95.2%, respectively; 1, 25 (OH_2) vitamin D increased to 84, 138 and 196, respectively. All three had dramatic clinical improvement in pain and weakness. Two subjects tolerated the procedure well with no complications; one had significant prolonged procedure-related localized pain. Although surgery remains the treatment of

Corresponding author: Michael T. Collins MD, Section on Skeletal Disorders and Mineral Homeostasis, National Institute of Dental and Craniofacial Research (NIDCR), National Institutes of Health (NIH), 30 Convent Drive, Room 228, MSC 4320, Bethesda, MD, 20892-4320, USA. Fax: 301-480-9962 fax, Phone: 301-436-4913, mc247k@nih.gov.

Disclosures: National Institutes of Health (NIH) and Philips have a cooperative research and development agreement (CRADA) and NIH has intellectual property in the field of “fusion” navigation system. Authors have nothing to disclose.

choice, cryoablation may be an effective, less invasive, and safe treatment for patients with difficult to remove tumors or who are poor surgical candidates.

Keywords

Tumor-induced osteomalacia; TIO; cryoablation; FGF23

Introduction

Tumor-induced osteomalacia (TIO) is a paraneoplastic syndrome associated with fractures, bone pain, and muscle weakness[1]. The vast majority of cases are caused by fibroblast growth factor-23 (FGF23)-secreting mixed connective tissue mesenchymal tumors[2]. FGF23 is a phosphate and vitamin-D regulating hormone that acts at the proximal renal tubule cells inhibiting both NaPi-2a/NaPi-2c (sodium-phosphate) co-transporter and 25-Hydroxyvitamin D 1-alpha-hydroxylase and activity resulting in increased renal phosphate excretion and to a lesser extent decreased intestinal phosphate absorption[3]. While tumor resection is curative and the standard of care, tumors are typically small (often < 2 cm) and notoriously difficult to localize even after systematic evaluation[1]. Even when the tumor is identified, surgery is sometimes not an option or carries high risk for morbidity, due to tumor location or co-morbid conditions. Medical treatment of patients with unlocalized, unidentified, inoperable or widely metastatic tumors is problematic. It involves administration of active vitamin D and at least thrice daily phosphate, which is poorly tolerated due to diarrhea. Frequent monitoring with careful adjustment of medications is required to prevent untoward effects of medical therapy, including secondary/tertiary hyperparathyroidism, hypercalcemia, hypercalciuria, nephrocalcinosis, and nephrolithiasis. A less invasive treatment option for inoperable phosphaturic mesenchymal tumors is image-guided cryoablation. Cryoablation induces tissue destruction by super-freezing. Multi-modality imaging guides the treatment needles in real-time. Ultrasound and CT guidance are augmented by fusion of MRI, FDG-PET/CT, or DOTATATE-PET/CT scans, depending upon which modality best defines the tumor margins. Fusion guidance involves segmentation of the tumor, co-registration and co-display of several imaging modalities, and real-time navigation with multi-modality feedback to guide the treatment needle to a location that will thermally destroy the tumor.

Herein, we report successful ablation in three subjects with clinical and biochemical evidence of TIO caused by mesenchymal tumors that were identified by systematic evaluation, but not operable, either due to high operative risk or anatomical location.

Subjects and Methods

The protocols were approved by the institutional review board, and informed consent was obtained from all subjects for the TIO protocol and for the fusion ablation protocol. Three subjects with the diagnosis of TIO underwent cryoablation of suspected PMTs. TIO was confirmed by a typical clinical history, absence of family history and negative gene testing of hereditary hypophosphatemic disorders, and biochemical confirmation based on hypophosphatemia, renal phosphate wasting, low or inappropriately normal serum

1,25(OH_2) Vitamin D, and an elevated serum FGF23 levels. The subjects were 58-, 72-, and 24-years old, and had been experiencing symptoms of hypophosphatemia for 10, 5, and 5 years, respectively. The details of clinical history, physical examination, biochemistry, and functional and anatomic localization studies were reviewed for each subject (Table 1).

Biochemical assays

Subjects who were being treated with phosphate and calcitriol discontinued therapy 6–14 days prior to the diagnostic evaluation; medications were restarted after the biochemical diagnosis of FGF23-mediated hypophosphatemia was confirmed. A detailed biochemical evaluation included blood phosphorous, alkaline phosphatase, calcium, creatinine, albumin, 25-hydroxyvitamin D, 1,25(OH_2) Vitamin D, PTH, tubular reabsorption of phosphate (%TRP), and intact FGF23. Tubular resorption of phosphate was measured from spot fasting urine and serum phosphorus and creatinine at baseline. FGF23 was assessed by ELISA (FGF23 [intact] kit; Immutopics, Inc, Athens, OH). This assay has a sensitivity of 3 pg/mL. The intra- and inter assay coefficients of variation are ≤ 3% and ≤ 4%, respectively.

Imaging and selective venous sampling

Octreotide SPECT/CT scan

A full body Octreotide SPECT/CT scan, including the head, hands, and feet, with imaging at 4 and 24 hours after IV administration of approximately 6 mCi (222 MBq) of ^{111}In-pentetreotide was performed in each subject. Low-dose, non-contrast CTs were used for attenuation correction and anatomic localization.

^{68}Ga-DOTATATE PET/CT scan

Through a peripheral vein, approximately 5 mCi of ^{68}Ga-DOTATATE was administered. After 60 minutes, the subject was positioned in the supine position in a PET/CT scanner (Siemens mCT), and full body images, including the head, hands, and feet, were obtained. A low-dose, non-contrast CT was used for attenuation correction and anatomic localization. Maximum standardized uptake values (SUVmax) were normalized by body weight.

FDG –PET/CT scan

Subjects were fasted for approximately 6 hours prior to IV injection with 5 to 10 millicuries 18F-FDG. Approximately one hour later, full body images, including the head, hands, and feet were obtained. Fasting blood glucose was <180–200 mg/dL. A low-dose, non-contrast CT was used for attenuation correction and anatomic localization. Maximum standardized uptake values (SUVmax) were normalized by body weight.

Anatomical imaging

Anatomical characterization of the suspected lesions was done using CT and/or MRI scans. CT scans with contrast were obtained on a 384-slice SOMATOM Force CT scanner (Siemens Healthcare), whereas MRI scans with contrast were performed on a 3 Tesla Siemens Sonata MR scanner (Siemens Medical Solutions, Inc). All imaging studies were analyzed and correlated with clinical information in a multidisciplinary team approach

(endocrinologists, nuclear medicine physicians, radiologists, interventional radiologists and orthopedic surgeons) to determine the optimal treatment options.

Intact FGF23 venous sampling

Confirmatory selective venous catheterization and sampling was done under fluoroscopic guidance for FGF23 measurements by an experienced interventional radiologist (RC) at the National Institutes of Health[4]. The catheter was inserted through the femoral or internal jugular vein. A mean of seventeen major veins and their branches were sampled. Between twenty-five and forty-nine 1.5- to 2-mL samples per subject (mean 31 samples) were taken from different locations.

Multimodality image-guided cryoablation

Cryoablation (Endocare, Healthronics) was used to induce tissue destruction by deep freezing with needles, with gases that change phase endothermically to reduce temperatures to below – 40 degrees C, which causes endothelial injury, apoptosis, and direct cellular injury from ice crystal formation[5]. A 17G needle(s) is placed in the suspected region of the tumor. Fusion guidance requires segmentation of the tumor pre-procedure, followed by intraprocedural co-registration and co-display of several imaging modalities, depending upon which modality defines the tumor and tumor margins best. The real-time navigation with multi-modality feedback facilitates operator manual guidance of the treatment needle to the location that will thermally destroy the tissue in the expected region of the previously-imaged tumor, using real time feedback of needle location in relation to the pre-operative imaging that localized the tumor. Fusion software and hardware are derivatives relying upon electromagnetic tracking platforms[6].

Results

In all three subjects, the suspect PMT was localized on either DOTATATE PET/CT or octreoscan SPECT/CT, and/or FGD-PET/CT, and confirmed on anatomical imaging with CT and MRI, as well as selective venous sampling for intact FGF23.

Subject 1 was a 58-year-old African American woman with past medical history of severe kyphosis, sternal deformity (Figure 1), and chronic obstructive pulmonary disease (COPD). She presented with a 10-year history of progressive, diffuse bone pain, muscle weakness and multiple fractures, limiting her ability to perform activities of daily living. She was essentially bed-bound, unable to transfer or walk without assistance and required a wheelchair for ambulation. The subject was treated with thrice daily phosphorous and calcitriol supplements with minimal benefit. She was referred to the NIH for tumor localization and management. Her baseline characteristics are summarized in Table 1. Of note, the subject had secondary/tertiary hyperparathyroidism (PTH: 518.2 pg/ml), thought to be secondary to FGF23-suppressed 1, 25 (OH_2) vitamin D levels. Octreotide SPECT/CT scan and FDG-PET/CT showed a small focus adjacent to the metal prosthesis in the left proximal femur. CT scan of the torso showed diffuse abnormal bone mineralization and several focal abnormalities suspicious for tumor causing TIO. CT and MRI studies of left femur were inconclusive due to extensive metallic artifact due to femoral neck and shaft

fixation. To better localize the culprit lesion, FGF23 venous sampling was performed. It confirmed the location of the tumor in the left proximal femur (Figure 1). She was a poor surgical candidate given her severe kyphosis and restrictive lung disease. CT-guided cryoablation under local anesthesia was performed (Figure 2). Cryoablation resulted in a rapid decrease in plasma intact FGF23 by 24-hours post-procedure (0 pg/ml), and correction of hypophosphatemia by post-procedure day #3 (2.7 mg/dl). Day # 3 renal tubular reabsorption of phosphate increased to 76% with corresponding rebound of 1,25(OH_2) Vitamin D_3 levels to 84 ng/dl (Figure 3). The subject tolerated the procedure well without any immediate complications, and had a dramatic clinical improvement in baseline pain and weakness. She has since experienced further clinical improvement and is now able to ambulate without assistance, drive a car, and carry out activities of daily living. Her most recent laboratory tests (6 months after the procedure) include phosphorous of 3.9 mg/dl, 1, 25 (OH_2) vitamin D of 98 pg/ml (%TRP: 78.73) and PTH of 281 pg/ml. The suspected tertiary hyperparathyroidism, remains to be addressed.

Subject 2 was a 72-year-old Caucasian female with a history of obstructive sleep apnea, diabetes mellitus type 2, cervical spine posterior longitudinal ligament calcification, cervical spine stenosis status post-surgical correction and left hip replacement surgery. She had a 5-year history of muscle weakness, fatigue, multiple fractures, and enthesopathy. Management of her hypophosphatemia prior to coming to NIH included phosphate, calcitriol, and cholecalciferol. Initial biochemical evaluation is summarized in table 1. Additional findings of note in this subject included calcified dura mater and calcified posterior longitudinal ligament in cervical spine area (figure 4) – both of which have not been previously reported in TIO, but can be seen in aged patients with XLH, suggesting this subject's TIO had been long-standing. While TIO was the most likely diagnosis, a genetic cause of FGF23-mediated hypophosphatemia was considered, due to a history of enthesopathies and ossifications of the posterior longitudinal ligament and calcified dura mater. Genetic testing for mutations in *PHEX*, *FGF23*, and *ENPP1* were negative. FDG-PET/CT scan showed a highly suspicious focus in the anterior cortex of the left proximal femoral shaft anterior to the surgical prosthesis, and a second, less suspicious hypermetabolic focus anterior to the right femoral neck (Figure 4). Octreotide SPECT/CT confirmed a probable neuroendocrine tumor in the anterior cortex of the left proximal femur. CT and MRI of the femurs showed an enhancing lesion along the anterior cortex of the proximal left femur measuring 0.8 cm × 0.4 cm. Venous sampling revealed a significant step-up in intact FGF23 at the site of the suspected lesion in the left femur, with the highest measurement of 195 pg/mL compared with levels around 90 pg/mL at other sites (Figure 4) Treatment options were discussed including surgical, and medical management. Given her multiple co-morbidities and the surgical difficulty and risks associated with tumor removal, the team and the subject opted for cryoablation which was performed without complications. Cryoablation resulted in a rapid decrease in intact FGF23 by 24-hours post-procedure to 2 pg/ml, and correction of the hypophosphatemia by day 3 post-procedure to 4.4 mg/dl. Day # 3 renal tubular reabsorption of phosphate increased to 94% and 1,25(OH_2) Vitamin D rebounded to 138 ng/dl. She had a dramatic clinical improvement in terms of generalized body pain and weakness after the surgery. However, one week after the ablation, she had insidious onset of left thigh pain, temporally and spatially related to cryoablation, without a clear radiologic change or

correlative mechanistic cause. Imaging failed to show any fluid collection or abnormal muscular soft tissue signal in the path of the cryoablation probe (MRI), no femoral diaphyseal periosteal reaction/fracture or major nerve in the probe insertion path. Only a thin cortical defect was seen in the anterior left femoral diaphysis, an expected result of cryoablation needle placement. Follow-up laboratory results 5 months after the procedure included phosphorous of 4.4 mg/dl (%TRP: 98.68) and 1, 25 (OH_2) vitamin D of 98 pg/ml.

Subject 3 was a 24-year-old Caucasian male who presented with progressively worsening right hip, knee and femur pain, and gait imbalance for 5 years. His symptoms progressed to include bilateral calf muscle cramps with weight bearing and proximal muscle weakness such that he was wheelchair-dependent within 4 years of symptom onset. Hypophosphatemic osteomalacia was eventually diagnosed and he was referred to the NIH for further evaluation. Initial biochemical evaluation is summarized in table 1. Skeletal radiographs revealed features of osteomalacia, with numerous fractures of varying stages throughout the skeleton. FDG-PET/CT showed suspicious mild abnormal uptake in the right ischium and acetabular region with bony changes and increased uptake in multiple muscle groups. Octreotide SPECT/CT scan showed no definite abnormalities but questionable foci in the right hand and pelvis. Therefore, a DOTATATE-PET/CT scan was performed, which revealed a lesion highly suspicious for a FGF23-secreting tumor in the right posterior inferior acetabulum (Figure 5). CT of the chest, abdomen and pelvis showed healed or healing rib fractures and scattered bone lucencies, as well as an elongated sclerotic focus in the area of the right ischium and acetabulum without evidence of a soft tissue neoplasm. MRI of the pelvis (Figure 5) confirmed enhancing masses within the right ischium (2.4 × 1.4 cm). A second focus, a hyper-intense lesion in the right lesser trochanter, with a low level of suspicion for malignancy, but possibly representing a second focus of disease, was noted. He subsequently underwent fluoroscopic sampling of the veins draining the hips and pelvis that showed FGF23 levels from 1400 to 1800 pg/mL from the right internal iliac, right internal gluteal, as compared to 200 to 450 pg/mL in the left internal iliac, left internal gluteal, right and left circumflex femoral (Figure 3). This confirmed the ischial lesion as the culprit lesion and the femoral lesion was excluded (due to super local venous sampling at femoral lesion site). The location of the tumor would have required an extensive resection of the acetabulum and part of the ischium, which would have resulted in significant morbidity for a young man. After thorough discussion with the multi-disciplinary team/tumor board, it was decided to proceed with an embolization and ablation procedure instead of resection. Given the large size of the tumor (2.4 × 1.4 cm), and to decrease post-operative morbidity, fluoroscopy-guided embolization of branches off the right internal iliac was performed 1 day prior to cryoablation. The subject tolerated the embolization procedure well, and was transferred to the Intensive Care Unit for overnight observation and close monitoring of his phosphorus levels, with the anticipation of acute hypophosphatemia due to possible post-embolization FGF23 surge. Prior to embolization, the subject had a phosphorus level of 1.7 mg/dL and calcium 2.14 mmol/l, with ionized calcium 1.15 mmol/L. Post-embolization, serum phosphorus and FGF23 were checked every 2 hours, which was then advanced to every 4 hours. The lowest serum phosphorus level was 1.5 mg/dL, 3 hours following embolization, which was corrected with an intravenous (i.v.) sodium phosphate infusion over 6 hours. Following the i.v. infusion of sodium phosphate, the serum phosphorus level

normalized and remained stable between 3.3 and 3.6 mg/dl. On the subsequent day, the subject had cryoablation of the ischial lesion under ultrasound and CT fusion guidance (Figure 2), with protective hydro-dissection of the sciatic nerve. He tolerated the procedure without any complications. Cryoablation resulted in a rapid decrease in plasma intact FGF23 by 24-hours post-procedure (9 pg/ml), and correction of the hypophosphatemia by post-procedure day #3 (3.6 mg/dl). Day #3 renal tubular reabsorption of phosphate and 1,25(OH_2) Vitamin D levels were increased to 95.2%, and 196 pg/ml, respectively (Figure 3). The subject had dramatic clinical improvement in baseline pain and weakness with no complications. He had a significant clinical improvement after the ablation and he is now able to carry out activities of daily living. His most recent labs (6 months after the procedure) include phosphorous of 3.4 mg/dl (%TRP: 95.36), 1, 25 (OH_2) vitamin D of 76 pg/ml.

Discussion

We describe three subjects who had clinical and biochemical evidence of TIO in whom the culprit tumor was localized by a combination of functional and anatomical imaging studies followed by confirmatory selective venous sampling. While the standard of care is surgical resection of culprit tumors, all three subjects were poor candidates for surgery due to the tumor location and/or co-morbidities. This led to the consideration of other, non-operative treatment options. In general, treatment options with fewer risks and side effects continue to expand for subjects with inoperable tumors. One emerging treatment option is minimally invasive, image-guided tumor ablation. With this form of treatment, individual tumors are destroyed using heat (radiofrequency, microwave, focused ultrasound, or laser ablation), cold (cryoablation) or chemical agents (percutaneous ethanol instillation). In general, ablative therapy is most often performed for tumors involving the liver, kidney, lung, and painful tumors of the bone. The goal of ablative therapy is most often complete tumor destruction, although pain palliation or immune stimulation are more recent indications that may not require complete ablation to be effective. Ablation is used as one of the preferred modalities of treatment in the management of soft tissue tumors such as osteoid osteoma, allowing rapid recovery with significantly shorter hospitalization[7].

The successful use of radiofrequency ablation for TIO with one year of follow-up was described by Hesse et al, in 2007[8]. Similar positive results with radiofrequency ablation were reported by Jadhav et al, who described short term resolution of TIO in two out of three patients[9]. In the patient who was not cured, the culprit lesion was large (5.6 × 6.5 cm). This trend for size to dictate ablation efficacy for local control has been seen in liver, lung, and kidney as well. Because of this, and because of the high vascularity of these tumors, we chose to combine both embolization and cryoablation in our patient with a lesion > 2cm. Highly vascular tumors are predisposed to convective heat gain during cryoablation (or convective heat loss during heat ablation). Both processes have the potential to distort the tumor in such a way as to diminish the efficacy of ablation. Tutton et al., were the first to describe image-guided ethanol with cryoablation for TIO[10]. In this case, a combination of ethanol injection and cryoablation was used with successful biochemical resolution and marked clinical improvement with 12 months of follow-up. For unstated reasons, Maybody et al., chose image-guided biopsy and cryoablation over surgery of a TIO tumor that was

peripherally located in lateral segment of the sixth rib. At six-week follow-up, there was no evidence of recurrence or tumor seeding from the biopsy[11]. Similarly, Cowan et al chose CT-guided cryoablation over surgery in a 25-year-old male who had a potentially resectable 1.8 cm PMT in the distal thigh[12]. No biochemical follow-up was reported beyond the period immediately following the procedure. Which procedure or combination of procedures to use in a specific situation is dictated by many factors including size and vascularity of tumor, local resource availability, and other factors. One feature of cryoablation that makes it attractive is the fact that as the tissue is frozen a visualizable “ice ball” is created that allows the person performing the procedure to be confident that freezing field encompasses the entire target mass.

The need for surgical resection with wide, clear margins as the preferred treatment method needs to be emphasized. Late recurrence of TIO, at times with widespread metastases is possible, and is a difficult, if not impossible to treat (reviewed in [1]). It is likely that recurrence is possible when very few tumor cells are left behind. For this reason, biopsies, with the attendant risk of tumor seeding, should also be avoided and only reserved for cases of significant uncertainty. Surgery, which yields tissue for diagnostics and scientific investigation, is even more important in the evolving era of tumor genomics. Tumor tissue affords the ability not only to study and understand the genetic and molecular pathogenesis of the tumor, but may also offer additional treatment options. This is already true with TIO and PMTs. The recent discovery of pathogenic fibronectin- and fibroblast growth factor 1-fibroblast growth factor receptor 1 translocations in a large subset of PMTs[13] has already led to treatment for inoperable TIO with the FGFR inhibitor BGJ398 (Novartis, Basel, Switzerland)[14].

In this series, two of the three subjects tolerated the procedure well without any immediate complications. One subject (#2) had localized pain at the site of the procedure that started within a week after the procedure. An obvious limitation of this series is the small sample size. However, this is expected given that TIO is a rare disease and only a minority of patients in whom tumors are localized will require non-surgical treatment. A novel feature of this study is that it is the first to describe fusion guidance for targeting the culprit lesion using nuclear medicine and PET scans, facilitated by the specificity of DOTATATE, octreotide, and FDG imaging with support from selective venous sampling. This approach allows for the precise targeting of very small tumors, as was the case in subject #2 whose tumor was only 8X4 mm in diameter. It is also the first report of the successful use of embolization followed by cryoablation for larger TIO tumors, and the longest follow-up for procedures of this type.

In conclusion, we report three subjects with inoperable TIO, who have demonstrated biochemical resolution and marked clinical improvement after multimodality image-guided cryoablation. Long term follow-up is essential in these cases before this form of treatment can be considered curative. Recurrence following incomplete resection (residual tumor at the margins) can sometimes take years. Until that time, this approach should be reserved for inoperable cases.

Acknowledgments

This research was supported by the Intramural Research Program of the National Institute of Dental and Craniofacial Research (NIDCR), National Institutes of Health Center for Interventional Oncology and the Intramural Research Program of the National Institutes of Health (NIH).

Authors' roles: Sri Harsha Tella cared for subjects, collected, organized, analyzed and interpreted the data, wrote and revised manuscript. Hayet Amalou cared for subjects, and assisted in drafting and revising manuscript. Brad Wood cared for subjects, performed the cryoablation procedure and assisted in drafting and revising manuscript. Richard Chang performed selective venous sampling and assisted in drafting and revising manuscript. Clara C Chen interpreted nuclear medicine and radiology studies, analyzed data, assisted in manuscript drafting and revision. Michelle Millwood cared for subjects, collected and organized data. Michelle Millwood cared for subjects, collected and organized data. Lori Guthrie cared for subjects, collected and organized data. Sheng Xu cared for subjects and assisted in performing cryoablation. Elliot Levy cared for subjects and assisted in performing cryoablation. Venkatesh Krishnasamy cared for subjects and assisted in performing cryoablation. Rachel I. Gafni cared for subjects, assisted in manuscript drafting and revision., Michael T Collins conceived and designed study, cared for subjects, organized and interpreted data, wrote and revised manuscript. Sri Harsha Tella and Michael T Collins are responsible for the integrity of data analysis. All authors approve final version of manuscript.

References

1. Chong WH, Molinolo AA, Chen CC, Collins MT. Tumor-induced osteomalacia. Endocrine-related cancer. Jun; 2011 18(3):R53–77. Epub 2011/04/15. [PubMed: 21490240]
2. Razzaque MS. The FGF23-Klotho axis: endocrine regulation of phosphate homeostasis\. Nature reviews. Nov; 2009 5(11):611–9.
3. Shimada T, Hasegawa H, Yamazaki Y, Muto T, Hino R, Takeuchi Y, et al. FGF-23 is a potent regulator of vitamin D metabolism and phosphate homeostasis. J Bone Miner Res. Mar; 2004 19(3): 429–35. [PubMed: 15040831]
4. Andreopoulou P, Dumitrescu CE, Kelly MH, Brillante BA, Cutler Peck CM, Wodajo FM, et al. Selective venous catheterization for the localization of phosphaturic mesenchymal tumors. J Bone Miner Res Research Support, NIH, Intramural. Jun; 2011 26(6):1295–302. Epub 2011/05/26.
5. Chu KF, Dupuy DE. Thermal ablation of tumours: biological mechanisms and advances in therapy. Nature reviews Cancer. Mar; 2014 14(3):199–208. Epub 2014/02/25. [PubMed: 24561446]
6. Krucker J, Xu S, Venkatesan A, Locklin JK, Amalou H, Glossop N, et al. Clinical utility of real-time fusion guidance for biopsy and ablation. Journal of vascular and interventional radiology : JVIR. Apr; 2011 22(4):515–24. Epub 2011/03/01. [PubMed: 21354816]
7. Rosenthal DI, Hornicek FJ, Wolfe MW, Jennings LC, Gebhardt MC, Mankin HJ. Percutaneous radiofrequency coagulation of osteoid osteoma compared with operative treatment. The Journal of bone and joint surgery American volume. Jun; 1998 80(6):815–21. Epub 1998/07/09. [PubMed: 9655099]
8. Hesse E, Rosenthal H, Bastian L. Radiofrequency Ablation of a Tumor Causing Oncogenic Osteomalacia. New England Journal of Medicine. 2007; 357(4):422–4. [PubMed: 17652663]
9. Jadhav S, Kasaliwal R, Shetty NS, Kulkarni S, Rathod K, Popat B, et al. Radiofrequency ablation, an effective modality of treatment in tumor-induced osteomalacia: a case series of three patients. The Journal of clinical endocrinology and metabolism. Sep; 2014 99(9):3049–54. Epub 2014/06/25. [PubMed: 24960541]
10. Tutton S, Olson E, King D, Shaker JL. Successful treatment of tumor-induced osteomalacia with CT-guided percutaneous ethanol and cryoablation. The Journal of clinical endocrinology and metabolism. Oct; 2012 97(10):3421–5. Epub 2012/07/28. [PubMed: 22837186]
11. Maybody M, Grewal RK, Healey JH, Antonescu CR, Fanchon L, Hwang S, et al. Ga-68 DOTATOC PET/CT-Guided Biopsy and Cryoablation with Autoradiography of Biopsy Specimen for Treatment of Tumor-Induced Osteomalacia. Cardiovascular and interventional radiology. Sep; 2016 39(9):1352–7. Epub 2016/05/07. [PubMed: 27150801]
12. Cowan S, Lozano-Calderon SA, Uppot RN, Sajed D, Huang AJ. Successful CT guided cryoablation of phosphaturic mesenchymal tumor in the soft tissues causing tumor-induced osteomalacia: a case report. Skeletal radiology. Feb; 2017 46(2):273–7. Epub 2016/12/07. [PubMed: 27921126]

13. Lee JC, Su SY, Changou CA, Yang RS, Tsai KS, Collins MT, et al. Characterization of FN1-FGFR1 and novel FN1-FGF1 fusion genes in a large series of phosphaturic mesenchymal tumors. Mod Pathol. Nov; 2016 29(11):1335–46. [PubMed: 27443518]

14. Collins, MT., Bergwitz, C., Aitcheson, G., Blau, J., Boyce, AM., Gafni, RI., et al. Striking Response of Tumor-Induced Osteomalacia to the FGFR Inhibitor NVP-BGJ398 American Society of Bone and Mineral Research Annual Meeting; Seattle, WA. 2015. p. LB-SA0035 and SA

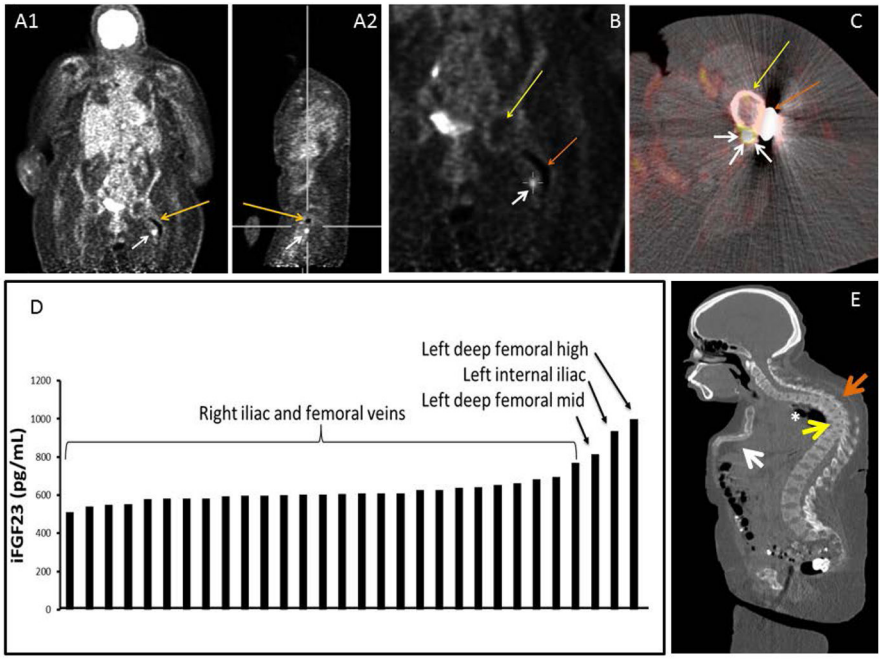

Figure 1.

Localization studies subject 1: Panel A. FDG-PET coronal (A1) and sagittal image (A2) showing artifact from rod (orange arrow) and culprit tumor (white arrow). Panel B: Coronal view of FDG-PET scan localizing the lesion (white arrow), femoral head (yellow arrow) and rod (orange arrow). Panel c: Axial view of FDG-PET/CT fusion imaging localizing the lesion-white arrows point the tumor, yellow arrow points the femoral shaft and orange arrow points the side plate. Panel D. Selective venous sampling for intact FGF23. There was a significant step-up in FGF23 concentration as the suspected tumor venous drainage was approached anatomically. Panel E. CT-Scan sagittal view showing sternal collapse (white arrow), kyphosis (orange arrow), vertebral compression fractures (yellow arrow) and restrictive lung disease (asterisk).

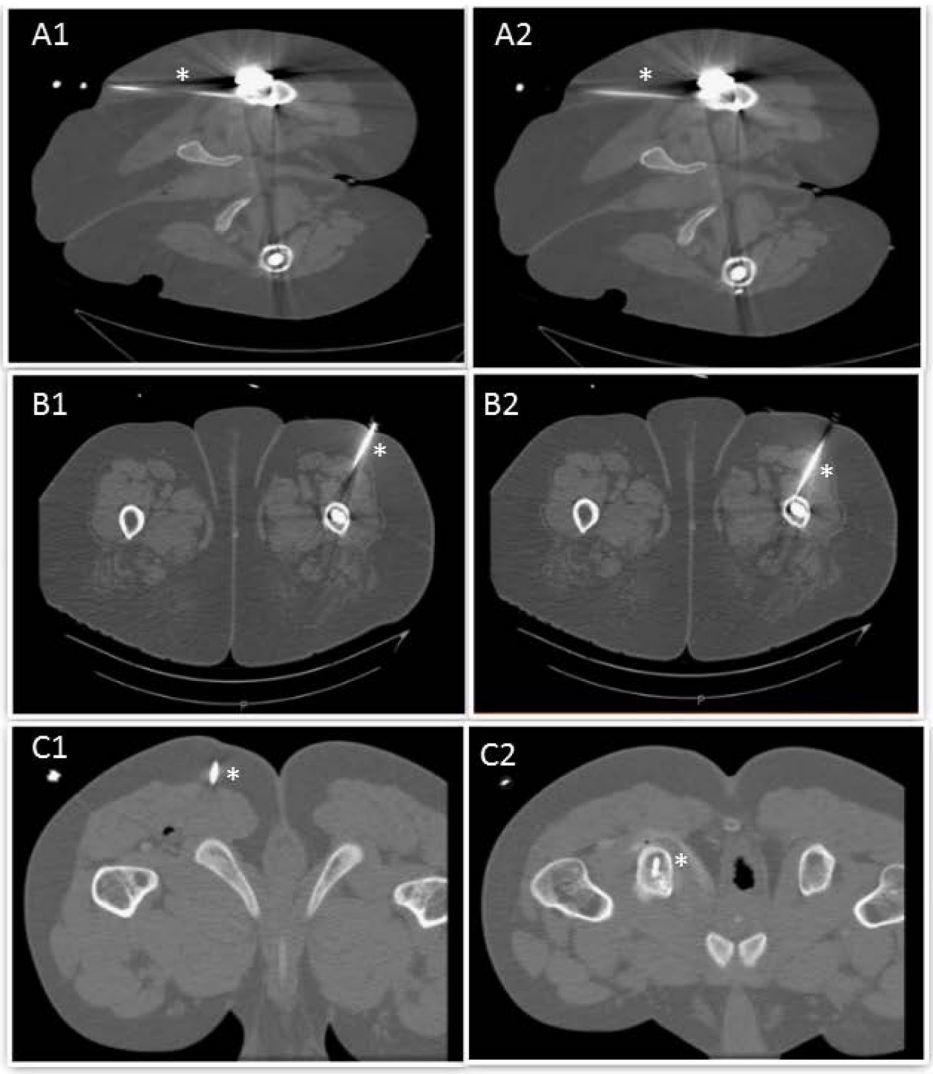

Figure 2.

Panels A1–A2 demonstrate cryoablation path in subject 1. Panels B1–B2 demonstrate cryoablation path in subject 2. Panels C1–C2 demonstrate cryoablation path in subject 3. * (asterisk) demonstrates cryoablation path in all the panels.

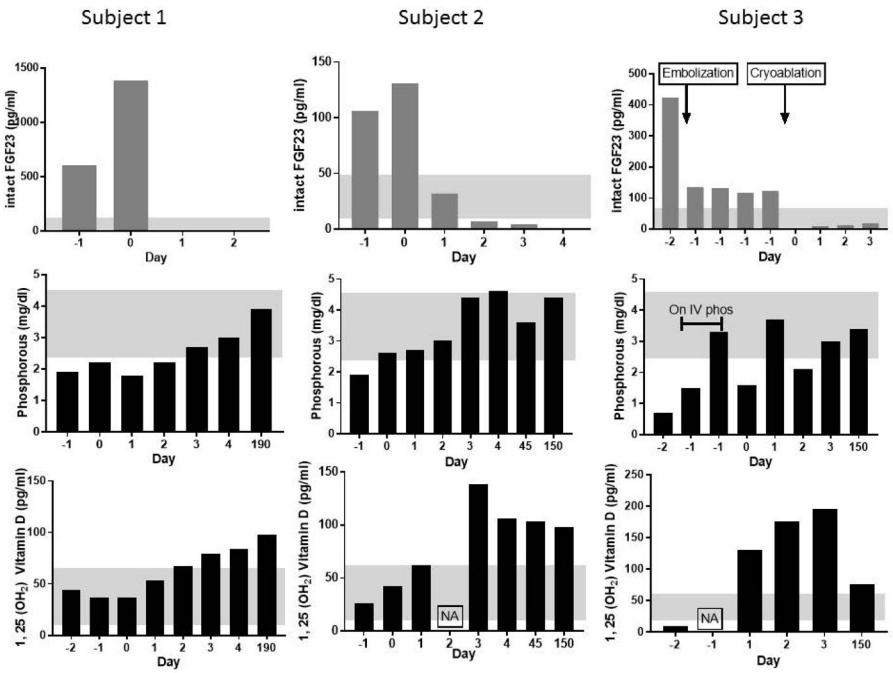

Figure 3.

Biochemical changes in response to treatment. iFGF23, Phosphorus and 1, 25 (OH_2) Vitamin D are plotted on vertical axis and day relative to the treatment is plotted on horizontal axis. In all the patients, iFGF23 levels dropped below the normal range by day 1 after cryoablation, Phosphorous returned to normal by day 3 and remained normal at follow up. 1, 25 (OH_2) vitamin D levels showed the typical supraphysiologic rebound that is seen in TIO after tumor removal. Subject 3, was the subject who underwent embolization prior to ablation, and showed a large decrease in FGF23 following embolization, which went to undetectable after cryoablation. The patient was placed on IV phosphate replacement overnight before proceeding to cryoablation.

Gray shadows indicate normal ranges. NA = Data not available.

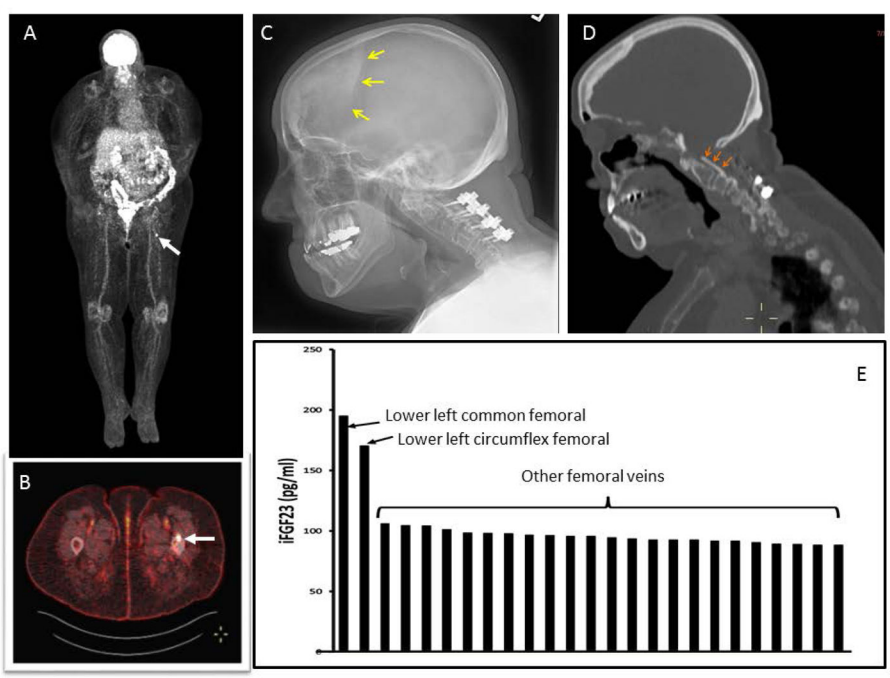

Figure 4.

Localization studies subject 2: Panels A, B: FDG PET demonstrating positive uptake in left proximal femur (white arrows). Panel C: Skull image demonstrating calcified duramater (yellow arrows). D. Orange arrows demonstrating calcified posterior longitudinal ligament in cervical spine area indicating the long-standing hypophosphatemia. E. Selective venous sampling for iFGF23. There was a significant step-up in iFGF23 concentration as the suspected tumor venous drainage was approached anatomically (lower left common and circumflex femoral veins).

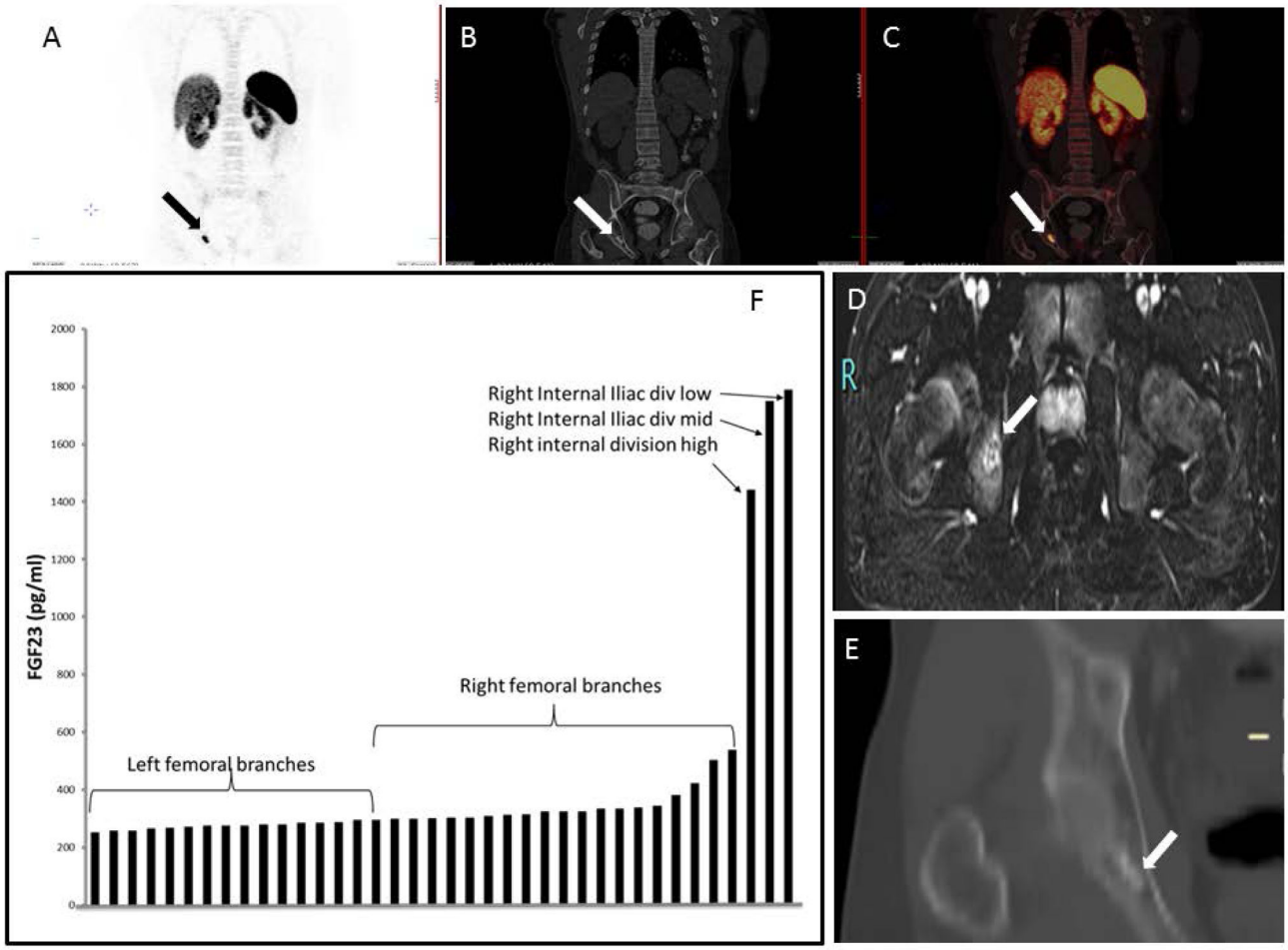

Figure 5.

Localization studies subject 3: Panels A, B, C: Ga^{68} DOTATATE isotopic uptake in right ischium corresponding to the right ischial mass. Panel D: MRI of the pelvis confirmed the ischial location. Panel E. CT scan coronal view of pelvis confirmed the lesion location in right ischium budding the acetabulum. Panel F. Selective venous sampling for intact FGF23. There was a significant step-up in FGF23 concentration as the suspected tumor venous drainage was approached anatomically.

Table 1

Baseline characteristics of subjects:

	Subject 1	Subject 2	Subject 3
Age (years)	58	72	24
Sex	Female	Female	Male
Duration of symptoms (years)	10	5	5
Pre-treatment Phosphorous (2.5–4.5 mg/dl)	1.8	1.5	0.7
Calcium (2.15–2.55 mmol/l)	2.37	2.54	2.20
Creatinine (0.51–0.95 mg/dl)	1.03	0.65	0.68
25-OH Vitamin D (> 30 ng/ml)	54	53	18
1, 25 $(OH)_2$ Vitamin D (18–64 pg/ml)	32	26	16
Intact FGF-23 (< 50 pg/ml)	1382	131	509
Pre-treatment TRP (%)	15.6	19.4	14
Pre-treatment Alkaline phosphatase (35–105 U/L)	242	106	429
PTH (15–65 pg/ml)	518.2	71.8	82.5
Octreotide SPECT/CT scan	Left proximal femur	Anterior cortex of left femur	Negative
FDG-PET/CT scan	Left proximal femur	Anterior cortex of left proximal femur prosthesis	Right ischium and acetabular uptake
DOTATATE-PET/CT scan	Not performed	Not performed	Right posterior inferior acetabulum
CT scan	Inconclusive[1]	Proximal femur	Right posterior inferior acetabulum
MRI scan	Inconclusive[1]	Proximal femur	2.4 × 1.4 right ischium mass
Length of follow-up	10 months	7 months	2 years 5 months

[1] Dedicated, CT and MRI were inconclusive due to artifact from metallic prosthesis, however, CT from both the Octreoscan SPECT/CT and FDG-PET/CT, when merged with isotopic imaging, could localize the lesion.